J. Appl. Comput. Mech., 8(4) (2022) 1287-1298
DOI: 10.22055/jacm.2022.39453.3411

ISSN: 2383-4536
jacm.scu.ac.ir

Shahid Chamran University of Ahvaz

Journal of Applied and Computational Mechanics

Research Paper

Thermomechanical Stresses of Multilayered Wellbore Structure of Underground Hydrogen Storage – A Simplified Solution Based on Recursive Algorithm

Lih Chi Sim[1], Wei Hong Yeo[1], Judha Purbolaksono[2], Lip Huat Saw[1], Jing Yuen Tey[1], Jer Vui Lee[1], Ming Chian Yew[1]

[1] Department of Mechanical and Material Engineering, Universiti Tunku Abdul Rahman, Jalan Sungai Long, Bandar Sungai Long, Cheras, 43000 Kajang, Selangor, Malaysia

[2] Department of Mechanical Engineering, Faculty of Industrial Technology, Universitas Pertamina, Jakarta 12220, Indonesia

Received December 14 2021; Revised March 10 2022; Accepted for publication March 10 2022.
Corresponding authors: J. Purbolaksono (yudha.purbolaksono@universitaspertamina.ac.id); W.H. Yeo (yeowh@utar.edu.my)

Abstract. Large scale of hydrogen storage is needed to balance the energy supply-demand fluctuation issues. Among few of the large scale storage systems, depleted oil and gas wells are widely employed. The construction of wellbore is normally in cylindrical shape and formed by layers of cement, casing and formation. As failure of wellbore is costly, proper structural integrity assessment is essential. In this article, an analytical solution derived based on recursive algorithm for estimating the thermomechanical stresses across the wellbore structure was proposed and verified. The temperature and stresses distribution results obtained from proposed analytical solution were compared with numerical results and they were found in good agreement. The percentage of difference was observed to be less than 0.1%. Besides that, a comparison study was performed on two, four and six layers wellbore structure. It was observed that four and six layers structure can produce much lower tangential tensile stress on the steel casing of the wellbore.

Keywords: Underground hydrogen storage, Multilayered wellbore, Thermomechanical stresses, Recursive method.

1. Introduction

In the effort to reduce carbon footprint and mitigate climate change, renewable energy use for power production has increased substantially in recent years [1-3]. As electricity generated from these renewable sources are often dynamic and intermittent, the success of integration of renewable energy sources in grid requires an efficient energy management and storage systems [4]. Many solutions have been proposed by researchers to overcome the intermittency [5-7]. Among them, conversion of surplus electric generated from renewable sources to hydrogen energy has been the promising solution to address demand-supply fluctuation issues. To make it feasible, underground storage system may appear to be a sensible solution for large scale of hydrogen energy storage, so that stored hydrogen can be used as fuel in a power plant during the peak load [8, 9].

Underground hydrogen storage is similar to underground gas storage and it can be done in underground gas storage infrastructure, therefore the experience and statistic in underground gas storage since year 1915 are important and relevant [10]. Depleted oil and gas fields have the potential to reduce cushion gas required for storage and it offered higher safety standard due to its previous construction [11]. The structure of oil and gas wellbore is typically constructed by layers of cement, casing and formations [12]. However, well use to store hydrogen appears to be more challenging because of phenomenon such as hydrogen embrittlement can cause adverse effect on the mechanical properties of casing material (steel) [9,13]. As failure of a large scale underground fuel gas storage is costly, a proper structural integrity assessment of well is important, so that safety margin can be accounted in the operation of the well [9, 14-16]. In the past, researchers have proposed various analytical methods to study the wellbore structure under different conditions. For example, Xie et al. [17] demonstrated the use of calliper survey data coupled with finite element analysis to study mechanisms of oil and gas well's casing collapse, buckling and shear. Manceau et al. [18] ran experiments on a one-to-one scale model of a wellbore in a rock laboratory to study different aspects of well integrity under different loadings. Shi et al. [19] proposed an analytical solution to estimate stress state of casing-cement-sheath formation with the consideration of initial loading and wellbore temperature variation under plane strain condition. Zhang et al. [20] performed analytical assessment on the underground gas storage cement's integrity by introducing cyclic loading to represent cyclic injection and production of the well. Bai et al. [21] developed a method that evaluate underground CO_2 storage well by using combined qualitative and quantitative analysis. The qualitative analysis consists of features, events and processes analysis while the quantitative analysis is represented by a mechanical model that shows the stress distribution within the casing/cement/rock composite wall. Song and Dan [22] performed finite element analysis on the casing joint and coupling section of an underground compressed natural gas (CNG) storage well.

Published online: March 20 2022

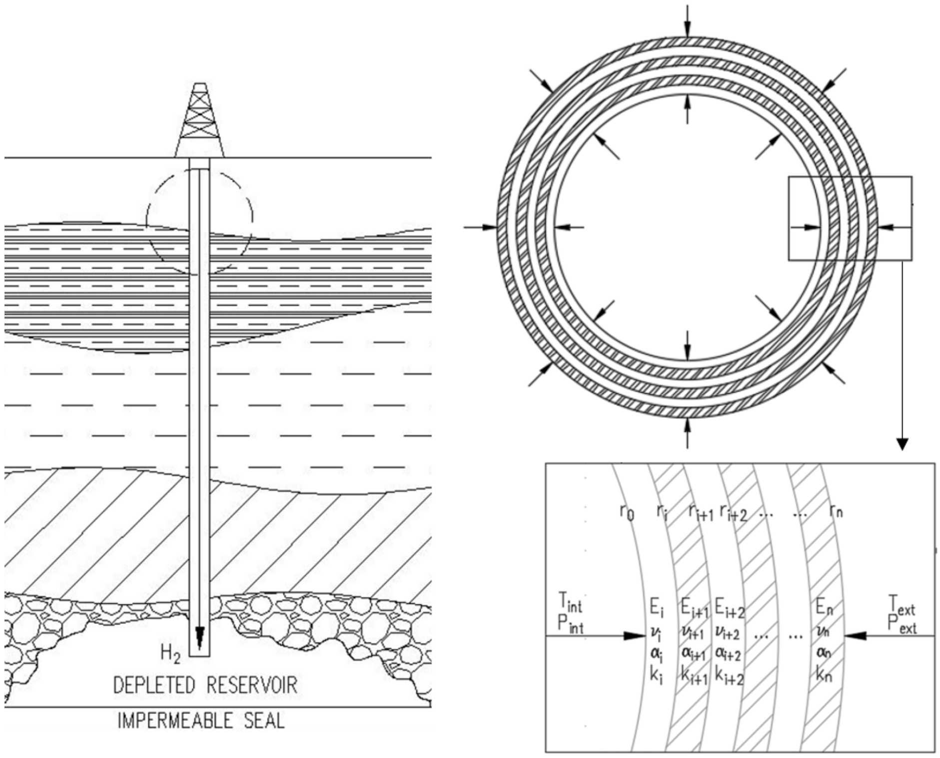

Fig. 1. Multilayered cylindrical wellbore structure that subjected to thermomechanical loading.

On the other hand, many researchers have explored the analytical techniques to analyze the thermomechanical of multilayered cylindrical problem. For example, Bakaiyan et al. [23] presented an exact elastic solution for thermal stresses and deformations of multilayered filament-wound composite pipes under internal pressure and temperature gradient. Lou et al. [24] developed a nonlinear theoretical model for calculating the tensile load under the boundary conditions of an arbitrary reinforced layer by using continuous displacement conditions, constitutive relation of elastic-plastic materials with the influence of thermal stress. The authors presented the model and used it to study the effect of temperature on tensile properties of reinforced thermoplastic pipe. He et al. [25] reported theoretical analysis for thermoplastic composite pipes under combined pure torsion and thermomechanical loading due to a constant surface temperature in the liner and convection to the seawater in the outer cover layer. Yeo et al. [26] modified the research works reported in Vedeld & Sollund [27] to obtain the exact solution for thermomechanical loaded multilayered hollow cylinder problem under plane strain assumption. As most analytical works reported in literatures are based on plane strain condition and analysis of oil and gas wellbore structure is often involved with uniform loading from structural weight above a wall section [19-21, 26, 28]. This paper aims to propose a reliable analytical solution for thermomechanical behavior of multilayered cylindrical wellbore structure under generalized plane strain condition which will consider for axial loading in the solution. The proposed analytical solution will be derived based on recursive algorithm and verified by comparing with thermo-elastic results produced from numerical analysis tool.

2. Heat Conduction and Stresses Equations for Multilayered Cylindrical Wellbore Structure under Thermomechanical Loading

2.1 Priori assumptions

The important assumptions used in this study are: (1) both temperature and pressure loadings on the well are constant; (2) the conduction heat transfer across the wall of wellbore structure is in a steady state condition; (3) small displacement and generalized plane strain conditions were applied when deriving the stress and displacement equations; (4) the multilayered cylindrical wellbore are perfectly bonded together for continuity of loadings.

2.2 Geometry and material properties

The multilayered cylindrical wellbore with n-layers is illustrated in Fig. 1. The inner and outer wall are subject to thermal and mechanical loading. The notations represents the outer radius of *i*-th layer. As shown in Fig. 1, material properties for *i*-th layer can be represented as follows, Poisson's ratio is ν_i, elastic modulus is E_i, thermal conductivity is k_i, and the thermal expansion coefficient is α_i.

2.3 Boundary and interface conditions

The inner and outer layers are subjected to temperature and pressure loadings. Based on the assumptions, the boundary and interface conditions for deriving the analytical solution can be identified. On the innermost and outermost surfaces, the boundary conditions can be written as $T_1(r_0)=\bar{T}_0=\bar{T}_{\text{int}}$, $\sigma_{rr,1}(r_0)=-p_0=-P_{\text{int}}$, $T_n(r_n)=\bar{T}_n=\bar{T}_{\text{ext}}$, $\sigma_{rr,n}(r_n)=-p_n=-P_{\text{ext}}$; where $\bar{T}_{\text{int}}$ and P_{int} are the temperature and pressure on the innermost surface; $T_1(r_0)$ and $\sigma_{rr,1}(r_0)$ represent the temperature and radial stress on the innermost surface of first layer; $\bar{T}_{\text{ext}}$ and P_{ext} are the temperature and pressure on the outermost surface, respectively; $T_n(r_n)$ and $\sigma_{rr,n}(r_n)$ indicate the temperature and radial stress on the outermost surface of *n*-th layer, respectively.

On the other hand, interface conditions in terms of temperature, heat flux, displacement and radial stress can be written as $T_i(r_i)=T_{i+1}(r_i)$, $q_i''(r_i)=q_{i+1}''(r_i)$, $u_{r,i}(r_i)=r_{r,i+1}(r_i)$, $\sigma_{rr,i}(r_i)=\sigma_{rr,i+1}(r_i)$, respectively.

2.4 Heat conduction equations

The governing equation of heat conduction in the cylindrical coordinates is generally written as,

$$k_i\left(\frac{\partial^2 T_i(r)}{\partial r^2}+\frac{1}{r}\frac{\partial T_i(r)}{\partial r}+\frac{1}{r^2}\frac{\partial^2 T_i(\varnothing)}{\partial \varnothing^2}+\frac{\partial^2 T_i(z)}{\partial z^2}\right)+\dot{R}_i=\rho_i c_i\frac{\partial T_i(t)}{\partial t} \tag{1}$$

where k, $\dot{R}$, ρ and c, respectively, denote the thermal conductivity, the internal heat generated per unit volume, the mass density and the specific heat [29]. In the absence of heat generation, the governing equation for one-dimensional steady state problem can be simplified as,

$$\frac{\partial}{\partial r}\left(r\frac{\partial T_i(r)}{\partial r}\right)=0 \tag{2}$$

Integrating Eq. (2), temperature equation can be obtained as,

$$T_i(r)=A_i+B_i\ln r \tag{3}$$

The heat flux equation can be written as,

$$\begin{aligned} q_i''(r)&=-k_i\frac{dT_i(r)}{dr}\\ q_i''(r)&=-k_i\frac{B_i}{r}\end{aligned} \tag{4}$$

In order to get the temperature distribution across any layer i, the integration constants A_i and B_i need to be identified by using the boundary and interface conditions. From interface condition of $T_i(r_i)=T_{i+1}(r_i)$ and $q_i''(r_i)=q_{i+1}''(r_i)$, the following two relations can be established,

$$A_i+B_i\ln r_i=A_{i+1}+B_{i+1}\ln r_i \tag{5}$$

$$k_i\left(\frac{B_i}{r_i}\right)=-k_{i+1}\left(\frac{B_{i+1}}{r_i}\right) \tag{6}$$

Rewriting Eq. (6) and Eq. (5),

$$A_{i+1}=A_i+B_i\ln r_i\left(1-\frac{k_i}{k_{i+1}}\right) \tag{7}$$

$$B_{i+1}=B_i\left(\frac{k_i}{k_{i+1}}\right) \tag{8}$$

Writing inner and outer interface temperatures of two adjacent layers,

$$A_i+B_i\ln r_{i-1}=\overline{T}_{i-1} \tag{9}$$

$$A_{i+1}+B_{i+1}\ln r_{i+1}=\overline{T}_{i+1} \tag{10}$$

Hence, by substituting Eq. (7) and Eq. (8) into Eq. (9) and Eq. (10), A_i and B_i can be written as follows,

$$A_i=\frac{\overline{T}_{i+1}x_i-\overline{T}_{i-1}y_i}{x_i-y_i} \tag{11}$$

$$B_i=\frac{x_i(\overline{T}_{i-1}-\overline{T}_{i+1})}{\ln r_{i-1}(x_i-y_i)} \tag{12}$$

where,

$$x_i=\delta_i\delta_{i+1} \tag{13}$$

$$y_i=\delta_{i+1}-\frac{k_i}{k_{i+1}}(\delta_{i+1}-1) \tag{14}$$

$$\delta_i=\frac{\ln r_{i-1}}{\ln r_i} \tag{15}$$

The temperature at outer radius of layer i is,

$$T_i(r_i) = A_i + B_i \ln r_i = \overline{T}_i \tag{16}$$

Putting Eq. (11) and Eq. (12) into Eq. (16) to obtain the relationship between temperatures at adjacent layers,

$$\overline{T}_{i+1} = \frac{\overline{T}_{i-1}(\delta_i y_i - x_i) + \overline{T}_i \delta_i (x_i - y_i)}{x_i(\delta_i - 1)} \tag{17}$$

Hence, for any layer i, constant A_i and B_i can be written in terms of inner and outer temperatures of the layer by using Eq. (11) and Eq. (12),

$$A_i = \frac{\overline{T}_i \delta_i - \overline{T}_{i-1}}{\delta_i - 1} \tag{18}$$

$$B_i = \frac{\delta_i(\overline{T}_{i-1} - \overline{T}_i)}{\ln r_{i-1}(\delta_i - 1)} \tag{19}$$

To determine A_i and B_i, it is necessary to write $\overline{T}_i$ in terms of defined boundary values $\overline{T}_0$ and $\overline{T}_n$. By introducing two simple recurrence relations,

$$a_{i+1} = \frac{a_{i-1}(\delta_i y_i - x_i) + a_i \delta_i (x_i - y_i)}{x_i(\delta_i - 1)} \tag{20}$$

$$b_{i+1} = \frac{b_{i-1}(\delta_i y_i - x_i) + b_i \delta_i (x_i - y_i)}{x_i(\delta_i - 1)} \tag{21}$$

where i = 1,2,3,… (*n*-1). Next, temperature $\overline{T}_i$ can be related to recurrence coefficients a and b as,

$$\overline{T}_i = a_i \overline{T}_1 + b_i \overline{T}_0 \tag{22}$$

Initial values of the recurrence coefficients can be set as,

$$a_0 = 0, a_1 = 1, b_0 = 1, b_1 = 0 \tag{23}$$

when i = *n*, $\overline{T}_1$ can be found through Eq. (22) and subsequently temperature *i* at all layer interfaces through Eq. (24),

$$\begin{gathered} \overline{T}_1 = \frac{\overline{T}_n - b_n \overline{T}_0}{a_n} \\ \overline{T}_i = \frac{a_i}{a_n}\overline{T}_n + \left(b_i - \frac{b_n}{a_n} a_i\right)\overline{T}_0 \end{gathered} \tag{24}$$

By using temperature i at all layer interfaces, constants A_i and B_i can be identified. Hence, the temperature at each radius point can be found by using Eq. (3).

2.5 Displacement and stresses equations for hollow cylindrical structure

The axisymmetric multilayered hollow cylinder section has varying temperature in radial direction with $\theta_i = T_i - T_r$ for T_r being the material initial temperature. Under small displacement and generalized plane strain conditions, the strain-displacement relations are as follows,

$$\epsilon_{rr,i} = \frac{du_{r,i}}{dr} \tag{25}$$

$$\epsilon_{\varnothing\varnothing,i} = \frac{u_{r,i}}{r} \tag{26}$$

$$\epsilon_{zz,i} = \frac{du_z}{dz} = C_z = \text{constant} \tag{27}$$

$$\epsilon_{r\varnothing,i} = \epsilon_{rz,i} = \epsilon_{\varnothing z,i} = 0 \tag{28}$$

$$\sigma_{rr,i} = \frac{E_i}{(1+v_i)(1-2v_i)}[(1-v_i)\epsilon_{rr,i} + v_i(\epsilon_{\varnothing\varnothing,i} + \epsilon_{zz,i}) - (1+v_i)\alpha_i \Delta_i] \tag{29}$$

$$\sigma_{\varnothing\varnothing,i} = \frac{E_i}{(1+v_i)(1-2v_i)}[(1-v_i)\epsilon_{\varnothing\varnothing,i} + v_i(\epsilon_{rr,i} + \epsilon_{zz,i}) - (1+v_i)\alpha_i \theta_i] \tag{30}$$

$$\sigma_{zz,i} = \frac{E_i}{(1+\upsilon_i)(1-2\upsilon_i)}[\upsilon_i(\epsilon_{\varnothing\varnothing,i}+\epsilon_{rr,i})+(1-\upsilon_i)\epsilon_{zz,i}-(1+\upsilon_i)\alpha_i\theta_i] \tag{31}$$

It is known that the equilibrium equation for axial symmetry in a multilayered cylinder is,

$$\frac{d\sigma_{rr,i}}{dr}+\frac{\sigma_{rr,i}-\sigma_{\varnothing\varnothing,i}}{r}=0 \tag{32}$$

By substituting Eq. (25) - Eq. (27) into Eq. (29) and Eq. (30), the equilibrium equation in terms of radial displacement, $u_{r,i}$ can be obtained as,

$$\frac{d}{dr}\left[\frac{1}{r}\frac{d(u_{r,i}r)}{dr}\right]=\frac{1+\upsilon_i}{1-\upsilon_i}\alpha_i\frac{d\theta_i}{dr} \tag{33}$$

By Integrating Eq. (33), the displacement under generalized plane strain condition can be written as,

$$u_{r,i}(r)=\beta_i C_i r+\lambda_i\frac{(D_i+I_i)}{r};\ u_{\varnothing,i}(r)=0;\ u_z(r)=C_z\frac{z}{L}=\epsilon_{zz}z \tag{34}$$

where,

$$I_i=I_i(r)=-\frac{E_i\alpha_i}{1-\nu_i}\int_{r_{i-1}}^{r}\theta_i r dr,\ \beta_i=\frac{(1+\nu_i)(1-2\nu_i)}{E_i},\ \lambda_i=-\frac{(1+\nu_i)}{E_i} \tag{35}$$

where C_i and D_i are the integration constants. Based on the Eq. (34), the stresses equations can be written in terms of C_i and D_i,

$$\sigma_{rr,i}(r)=C_i+\frac{D_i+I_i}{r^2}+\varphi_i;\quad \sigma_{\varnothing\varnothing,i}(r)=C_i-\frac{D_i+I_i}{r^2}+\varphi_i-\frac{E_i\alpha_i\theta_i}{(1-\upsilon_i)}\quad; \tag{36}$$

$$\sigma_{zz,i}(r)=2\nu_i C_i+\frac{(1-\nu_i)\epsilon_{zz}}{\beta_i}-\frac{E_i\alpha_i\theta_i}{(1-\upsilon_i)} \tag{37}$$

where $\varphi_i=\upsilon_i\epsilon_{zz}/\beta_i$. The thermal stresses across the multilayered cylindrical structure can be computed after obtaining the temperatures distribution at all interface points. By using the boundary and interface conditions of displacement and radial stresses across the structure, the constants C_i and D_i can be determined. By applying the interface conditions, following relation can be obtained,

$$C_i+\frac{D_i+I_i}{r_i^2}+\varphi_i=C_{i+1}+\frac{D_{i+1}+I_{i+1}^0}{r_i^2}+\varphi_{i+1} \tag{38}$$

$$\beta_i C_i r_i+\lambda_i\frac{(D_i+I_i)}{r_i}=\beta_{i+1}C_{i+1}r_i+\lambda_{i+1}\frac{(D_{i+1}+I_{i+1}^0)}{r_i} \tag{39}$$

where $I_{i+1}^0=I_{i+1}(r_i)=\frac{-E_{i+1}\alpha_{i+1}}{1-\upsilon_{i+1}}\int_{r_i}^{r_i}\theta_i r dr=0$; $I_i=I_i(r_i)=\frac{-E_i\alpha_i}{1-\upsilon_i}\int_{r_{i-1}}^{r_i}\theta_i r dr$.

Solving Eq. (38) and (39) to obtain C_{i+1} and D_{i+1},

$$\begin{aligned}D_{i+1}&=(D_i+I_i)\left(\frac{\lambda_i-\beta_{i+1}}{\lambda_{i+1}-\beta_{i+1}}\right)+C_i r_i^2\left(\frac{\beta_i-\beta_{i+1}}{\lambda_{i+1}-\beta_{i+1}}\right)+\beta_{i+1}r_i^2\left(\frac{\varphi_{i+1}-\varphi_i}{\lambda_{i+1}-\beta_{i+1}}\right)\\ C_{i+1}&=\left(\frac{D_i+I_i}{r_i^2}\right)\left(\frac{\lambda_{i+1}-\lambda_i}{\lambda_{i+1}-\beta_{i+1}}\right)+C_i\left(\frac{\lambda_{i+1}-\beta_i}{\lambda_{i+1}-\beta_{i+1}}\right)+\lambda_{i+1}\left(\frac{\varphi_i-\varphi_{i+1}}{\lambda_{i+1}-\beta_{i+1}}\right)\end{aligned} \tag{40}$$

Since it is assumed that the layers are perfectly bonded, the radial stresses of two adjacent layers are set to be equal to the corresponding contact pressure,

$$\begin{aligned}\sigma_{rr,i}(r_{i-1})=-p_{i-1}\ &=>\ C_i+\frac{D_i+I_i^0}{r_{i-1}^2}+\varphi_i=-p_{i-1}\\ \sigma_{rr,i+1}(r_{i+1})=-p_{i+1}\ &=>\ C_{i+1}+\frac{D_{i+1}+I_{i+1}}{r_{i+1}^2}+\varphi_{i+1}=-p_{i+1}\end{aligned} \tag{41}$$

where,

$$I_i^0=I_i(r_{i-1})=\frac{-E_i\alpha_i}{1-\upsilon_i}\int_{r_{i-1}}^{r_{i-1}}\theta_i r dr=0 \tag{42}$$

Substituting Eq. (41) into Eq. (40) yields,

$$D_i = \gamma_i r_i^2 \left(\frac{p_{i-1}G_i - p_{i+1}(\lambda_{i+1} - \beta_{i+1}) + \varphi_i (G_i + \beta_{i+1}\gamma_{i+1} - \lambda_{i+1}) - \varphi_{i+1}\beta_{i+1}(\gamma_{i+1} - 1)}{S_i - G_i} \right) - \frac{I_i S_i + I_{i+1}\gamma_i \gamma_{i+1}(\lambda_{i+1} - \beta_{i+1})}{S_i - G_i} \tag{43}$$

$$C_i = \frac{-p_{i-1}S_i + p_{i+1}(\lambda_{i+1} - \beta_{i+1}) - \varphi_i (S_i + \beta_{i+1}\gamma_{i+1} - \lambda_{i+1}) + \varphi_{i+1}\beta_{i+1}(\gamma_{i+1} - 1)}{S_i - G_i} + \frac{I_i S_i + I_{i+1}\gamma_i \gamma_{i+1}(\lambda_{i+1} - \beta_{i+1})}{r_{i-1}^2 (S_i - G_i)} \tag{44}$$

where $S_i = \gamma_i \gamma_{i+1}(\lambda_i - \beta_{i+1}) + (\lambda_{i+1} - \lambda_i)\gamma_i$; $G_i = \lambda_{i+1} - \beta_i + (\beta_i - \beta_{i+1})\gamma_{i+1}$; $\gamma_{i+1} = r_i^2 / r_{i+1}^2$

The contact pressure on the outer surface of i-layer can be expressed as,

$$\sigma_{rr,i}(r_i) = -p_i \quad => \quad C_i + \frac{D_i + I_i}{r_i^2} + \varphi_i = -p_i \tag{45}$$

Hence, substituting Eq. (43) into Eq. (45) to obtain the relation of the adjacent contact pressures as,

$$p_{i+1} = \frac{p_{i-1}(S_i - \gamma_i G_i) - p_i (S_i - G_i)}{(1-\gamma_i)(\lambda_{i+1} - \beta_{i+1})} - \frac{I_{i+1}\gamma_{i+1}(\lambda_{i+1} - \beta_{i+1})(1-\gamma_i) + I_i \left(\frac{S_i}{\gamma_i} - G_i \right)}{r_i^2 (1-\gamma_i)(S_i - G_i)} - \frac{(1-\gamma_{i+1})(\upsilon_i - \upsilon_{i+1}) \epsilon_{zz}}{(\lambda_{i+1} - \beta_{i+1})} \tag{46}$$

Next, substituting Eq. (46) into Eq. (43) gives constants D_i and C_i in terms of contact pressures,

$$D_i = \frac{\gamma_i r_i^2}{1-\gamma_i} \left(p_i - p_{i-1} + \frac{I_i}{r_i^2} \right) \tag{47}$$

$$C_i = \frac{1}{1-\gamma_i} \left(\gamma_i p_{i-1} - p_i - \frac{I_i}{r_i^2} \right) - \varphi_i \tag{48}$$

Two recurrence relations for recursive coefficients c_i and d_i can be proposed as below,

$$c_{i+1} = \frac{c_{i-1}(S_i - \gamma_i G_i) - c_i (S_i - G_i)}{(1-\gamma_i)(\lambda_{i+1} - \beta_{i+1})} \tag{49}$$

$$d_{i+1} = \frac{d_{i-1}(S_i - \gamma_i G_i) - d_i (S_i - G_i)}{(1-\gamma_i)(\lambda_{i+1} - \beta_{i+1})} - \frac{I_{i+1}\gamma_{i+1}(\lambda_{i+1} - \beta_{i+1})(1-\gamma_i) + I_i \left(\frac{S_i}{\gamma_i} - G_i \right)}{p_0 r_i^2 (1-\gamma_i)(S_i - G_i)} - \frac{(1-\gamma_{i+1})(\upsilon_i - \upsilon_{i+1}) \epsilon_{zz}}{p_0 (\lambda_{i+1} - \beta_{i+1})} \tag{50}$$

where i = 1,2,. . . , (n-1). Express p_i in terms of p_0 and p_1, a recurrence relation can be written as follows,

$$p_i = c_i p_1 + d_i p_0 \tag{51}$$

with the initial values of $c_0 = 0, c_1 = 1, d_0 = 1, d_1 = 0$. Since p_1 can be written as $p_1 = (p_n - d_n p_0)/c_n$, contact pressure at each interface p_i can be expressed as a function of the recurrence relations with boundary values as below,

$$p_i = \frac{c_i}{c_n} p_n + \left(d_i - \frac{d_n}{c_n} c_i \right) p_0 \tag{52}$$

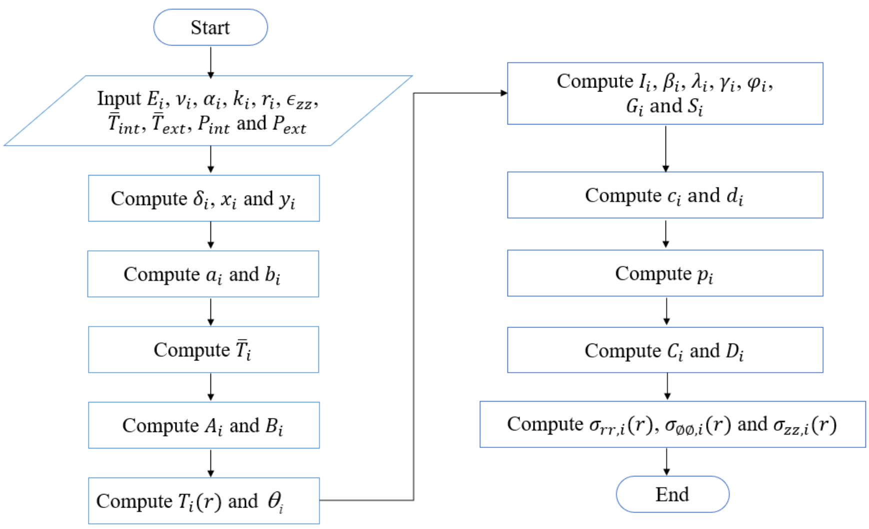

Fig. 2. Flow chart of computational procedure.

Table 1. Material properties [28]

Material	Young's Modulus, E (MPa)	Poisson's Ratio, ν	Heat Conductivity, k ($Wm^{-1}K^{-1}$)	Heat Expansion Coefficient, α (K^{-1})
Steel	2×10^5	0.2	45	1.1×10^{-5}
Cement	1.4×10^4	0.35	1.5	1.3×10^{-5}

Table 2. Geometry information and loadings subjected to the wellbore structure [28]

Geometry					Loadings			
Model	Layer	Material	Inner Radius (m)	Outer Radius (m)	Internal Pressure (MPa)	External Pressure (MPa)	Internal Temperature (°C)	External Temperature (°C)
2L	1	Steel	0.113	0.125	15	10	60	45
	2	Cement	0.125	0.155				

2.6 Computational Procedure

To estimate the temperature and stresses distribution across the multilayered cylindrical wellbore structure, a simple computational procedure can be implemented as below,

1. Determine the sequences of $\{x_i\}$, $\{y_i\}$ and $\{\delta_i\}$ following Eq. (13) to Eq. (15)
2. Compute the sequences $\{a_i\}$ and $\{b_i\}$ by using Eq. (20) and Eq. (21) with initial values from Eq. (23)
3. Identify sequences of $\{\bar{T}_i\}$ by using Eq. (24)
4. Calculate sequences of $\{A_i\}$ and $\{B_i\}$ by using Eq. (18) and Eq. (19)
5. Hence, temperature distribution can be obtained through Eq. (3) and the sequences of $\{\theta_i\}$ can be computed
6. Establish the sequences of $\{\beta_i\}$, $\{\lambda_i\}$, $\{\varphi_i\}$ and $\{I_i\}$.
7. Determine the sequences of $\{\gamma_i\}$, $\{G_i\}$ and $\{S_i\}$ in Eq. (11).
8. Compute the sequences of $\{c_i\}$ and $\{d_i\}$ by using Eq. (16) and (17) with initial values from Eq. (18).
9. Identify $\{p_i\}$ in Eq. (52).
10. After that, $\{C_i\}$ and $\{D_i\}$ can be determined from Eq. (47) and (48).
11. Lastly, stresses stated in Eq. (36) can be computed by using $\{C_i\}$ and $\{D_i\}$.

Figure 2 illustrates a computational procedure flow chart that shows the sequence of parameters to be computed to obtain temperature and stresses across the multilayered cylindrical wellbore structure.

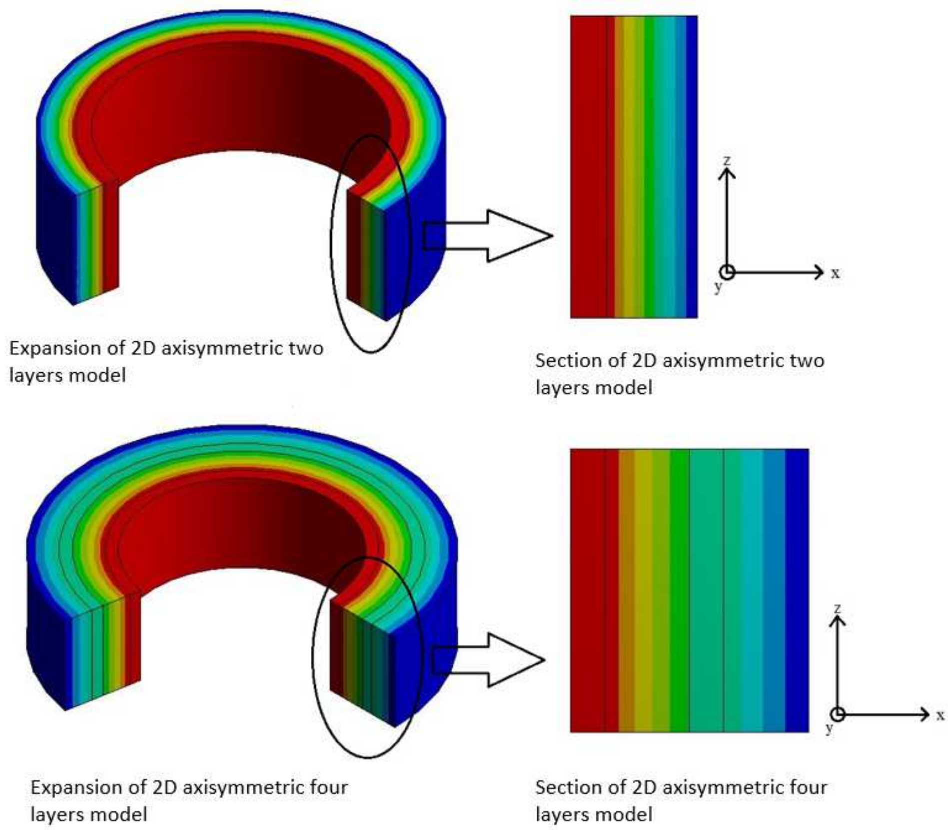

Fig. 3. Two-dimensional axisymmetric cylindrical FE models.

3. Results and Discussion

3.1 Validation of the proposed analytical solution

Validation of the proposed analytical solution is done by comparing generated results with those obtained from numerical simulation. A depleted gas well structure reported in Hartmann et al. [28] was used as model for validation studies. The wellbore design consists of two layers which formed by steel casing (as inner layer) and cement (as outer layer). Table 1 shows the respective material properties while Table 2 summarizes the model's geometry and loadings. The wellbore structure was modelled as a two-dimensional (2D) axisymmetric cylinder in finite element analysis (FEA) software ANSYS. Figure 3 illustrates the axisymmetric cylindrical FE models used in present work. In terms of meshing, the quadrilateral and PLANE13 elements with converged mesh size of 0.0001 m were applied to the model. The two layers were bonded together to ensure for mesh connectivity. Based on generalized plane strain assumption, a downward axial displacement of 0.005 mm was applied to the top boundary of the model wall section.

As shown in Fig. 4, the results of temperature distribution obtained from FEA are in-line with the results produced by using analytical solution. For the stress analysis, the Von Mises stress obtained from analytical solution can be written as $\sigma_{VM} = \sqrt{0.5[(\sigma_{rr} - \sigma_{\phi\phi})^2 + (\sigma_{\phi\phi} - \sigma_{zz})^2 + (\sigma_{zz} - \sigma_{rr})^2]}$ [31]. Figure 5 and 6 show the radial, tangential, axial and Von Mises stresses produced by both proposed analytical solution and FEA ANSYS. It is found that the results are in well agreement to each other. In general, the percentage of difference for temperature and stresses results produced by using the proposed analytical solution and FEA were recorded at less than 0.1%. Therefore, the proposed analytical solution based on recursive method can be a reliable alternative to numerical method. As analytical solution does not require meshing operation, the computing cost for solving a problem analytically is much lower as compared to numerical simulation. Besides that, the advantage of present proposed analytical solution will be noticeable especially when the number of layers increases.

3.2 Comparison of two layers with four and six layers wellbore structure

Depleted oil and gas wells are widely adopted for large scale hydrogen storage mainly because the facilities needed are not differ very much [6]. Over hundred years of development, guidelines for design and construction of oil and gas fields have improved for better quality of well. Codes such as NORSOK standard D-010 stated that an oil and gas wells should be designed to have double barrier to provide better isolation of formation fluid [32]. However, there may be some old oil and gas wells constructed before the establishment of these codes are having single barrier design [33]. As there is not much of research work that present the effect of number of layers on the thermal elastic behaviour of well, this section is to investigate the differences in terms of temperature distribution and stresses development between a two layers wellbore (single casing), four layers (double casing) and six layers (triple casing) wellbore under same loading conditions.

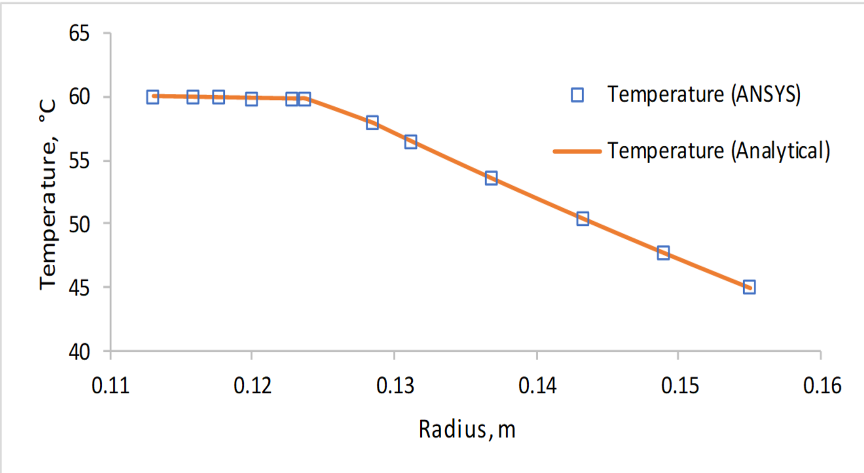

Fig. 4. Temperature distribution across the wellbore structure.

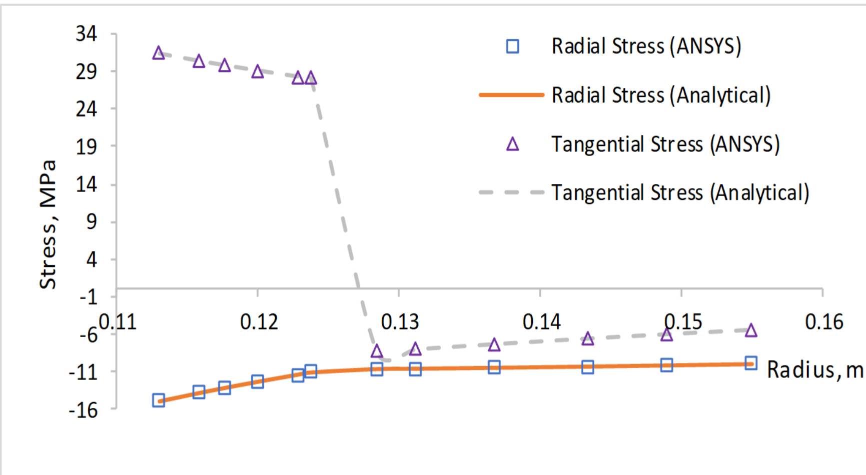

Fig. 5. Radial and tangential stresses across the wellbore structure.

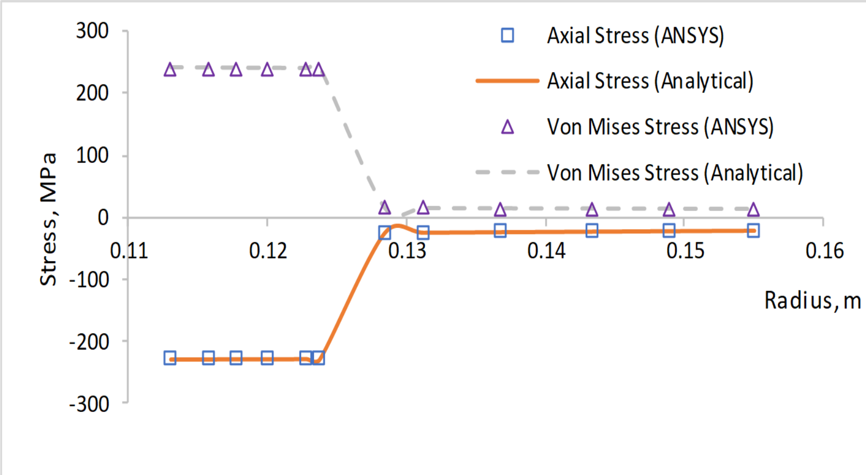

Fig. 6. Axial and Von Mises stresses across the wellbore structure.

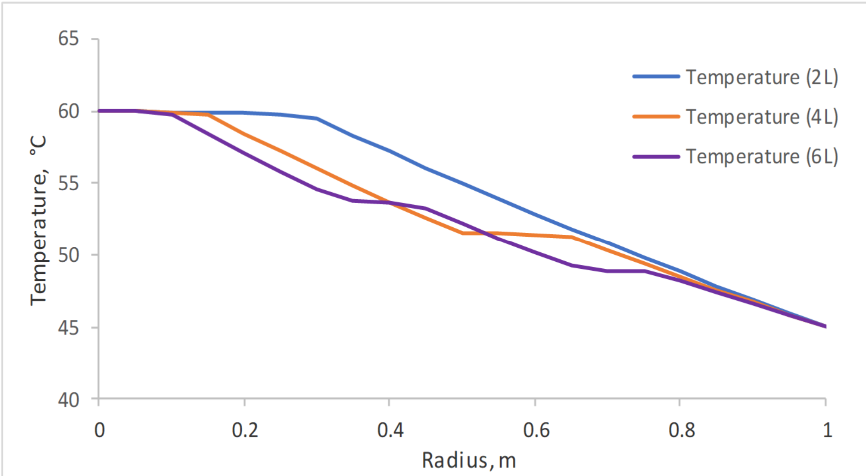

Fig. 7. Temperature distribution across two layers (2L), four layers (4L) and six layers (6L) wellbore structures.

A four- and six-layers wellbore with geometry stated in Table 3 were used for comparison with the 2 layers model reported in Table 2. The material properties and loadings of the four and six layers were modelled same as those stated in Table 1 and Table 2.

To enable a fair comparison, a dimensionless parameter $\zeta = (r - r_0)/(r_n - r_0)$ was introduced in the results presentation. Fig. 7 to 10 depict the temperature distribution and stresses development of the two, four and six layers wellbore. From the results, maximum tangential tensile stress across the four layers wellbore was found to be lower, 19.2MPa as compared to two layers wellbore, 31.4 MPa. It marked a reduction of 38.8% in the maximum tangential tensile stress. As the number of layers increased from four to six, the maximum tangential tensile stress was found to be further decreased. As for other stresses such as of radial, axial and Von-misses stresses, only marginal effect was observed. Besides providing additional layers to prevent gas leaking [16], the increasing number of layers can also reduce the tangential tensile stress which is the main stress component that often results in wellbore failure such as radial cracking [21]. As storage of hydrogen often demand for safe and high quality of wellbore structure, present analysis showed the design with four or more layers could be the favourable option.

Table 3. Geometry of four and six layers wellbore models

Geometry				
Model	Layer	Material	Inner Radius *(m)*	Outer Radius *(m)*
4L	1	Steel	0.113	0.125
	2	Cement	0.125	0.155
	3	Steel	0.155	0.167
	4	Cement	0.167	0.197
6L	1	Steel	0.113	0.125
	2	Cement	0.125	0.155
	3	Steel	0.155	0.167
	4	Cement	0.167	0.197
	5	Steel	0.197	0.209
	6	Cement	0.209	0.239

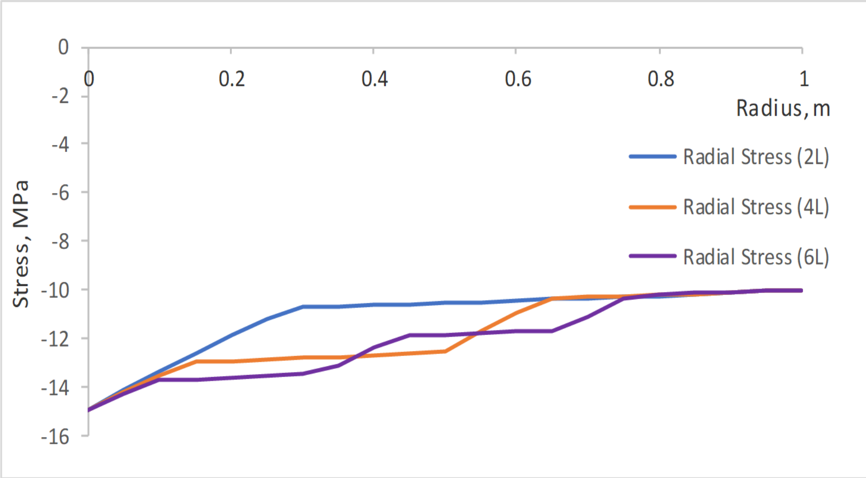

Fig. 8. Radial stress across two layers (2L), four layers (4L) and six layers (6L) wellbore structures.

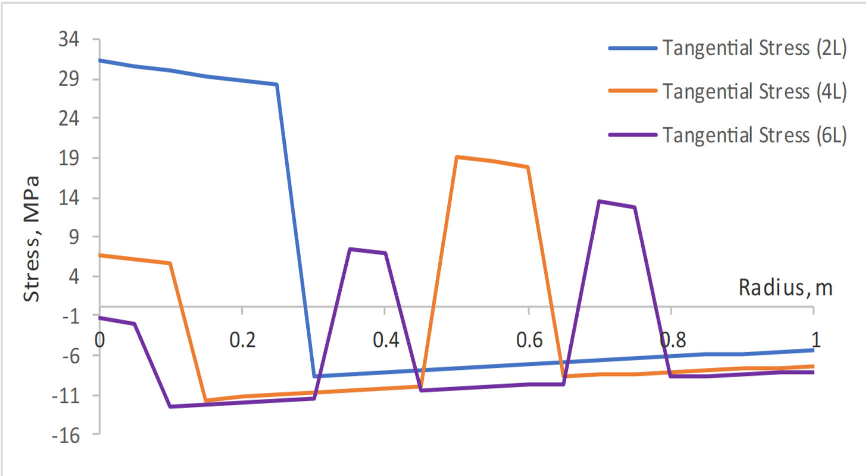

Fig. 9. Tangential stress across two layers (2L), four layers (4L) and six layers (6L) wellbore structures.

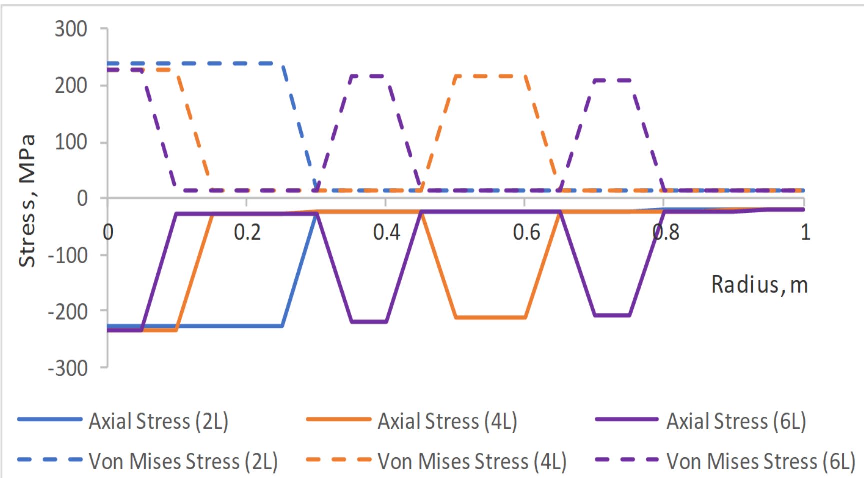

Fig. 10. Axial and Von Mises stresses across two layers (2L), four layers (4L) and six layers (6L) wellbore structures.

4. Conclusion

In this article, a reliable analytical solution to predict the thermomechanical stresses of multilayered wellbore structure has been formulated and verified. The thermoelastic results generated by using the present analytical solution and FEA were found in agreement to each other. Generally, the percentage of difference between proposed analytical solution and FEA was less than 0.1%. Also, a study of comparing two, four and six layers wellbore was performed by using the proposed analytical solution. It was demonstrated that four or more layers wellbore structure was found to be more suitable for hydrogen storage as it can reduce the maximum tangential tensile stress. In conclusion, the proposed analytical solution can be served as an efficient and inexpensive tool for wellbore integrity assessment.

Authors' Contributions

L.C. Sim was in-charged in the development of exact solution, validation and manuscript draft; W.H. Yeo, J. Purbolaksono and L.H. Saw were the supervisors and providing guidance, direction and editing of the work; J.Y. Tey, J.V. Lee and M.C. Yew assisted in proof read, validation and compilation work. The manuscript was written through the contribution of all authors. All authors discussed the results, reviewed, and approved the final version of the manuscript.

Acknowledgements

This work was supported by UTARRF Grant No. IPSR/RMC/UTARRF/2018-C2/Y02 from UTAR.

Conflict of Interests

The authors declared no potential conflicts of interest concerning the research, authorship, and publication of this article.

Funding

The funding was provided by Universiti Tunku Abdul Rahman Research Fund under Grant No. IPSR/RMC/UTARRF/2018-C2/Y02.

Data Availability Statements

The datasets generated and/or analyzed during the current study are available from the corresponding author on reasonable request.

Nomenclature

CNG	Compressed natural gas
CO_2	Carbon dioxide
E_i	Elastic modulus for i-th layer [Pa]
ν_i	Poisson's ratio for i-th layer [-]
α_i	Thermal expansion coefficient for i-th layer [$^\circ C^{-1}$]
k_i	Thermal conductivity for i-th layer [$Wm^{-1}\,^\circ C^{-1}$]
r_i	Outer radius for i-th layer [m]
r	Radial coordinate [m]
r_0	Inner radius for first layer [m]
r_n	Outer radius for outermost layer [m]
P_{int}	Pressure loading at inner surface of vessel [Pa]
P_{ext}	Pressure loading at outer surface of vessel [Pa]
$\overline{T}_{int}$	Temperature at inner surface of vessel [$^\circ C$]
$\overline{T}_{ext}$	Temperature at outer surface of vessel [$^\circ C$]
$\overline{T}_i$	Temperature at surface/interface points [$^\circ C$]
T_i	Temperature distribution for i-th layer [$^\circ C$]
q_i''	Radial heat flux for i-th layer [Wm^{-2}]
$u_{r,i}$	Radial displacement for i-th layer [m]
A_i	Integration constant for i-th layer
B_i	Integration constant for i-th layer
x_i	$=\delta_i\delta_{i+1}$ [-]
y_i	$=\delta_{i+1}-(k_i/k_{i+1})(\delta_{i+1}-1)$ [-]
δ_i	$=\ln r_{i-1}/\ln r_i$ [-]
a_i	Recursive relation; Defined by Eq. (20) [-]
b_i	Recursive relation; Defined by Eq. (21) [-]
ϕ_i	Polar angle coordinate
z	Axial coordinate [m]
θ_i	$=T_i-T_r$ [$^\circ C$]
$\epsilon_{rr,i}$	Radial strain for i-th layer [-]
$\epsilon_{\phi\phi,i}$	Tangential strain in azimuthal angle direction for i-th layer [-]
$u_{z,i}$	Axial displacement for i-th layer [m]
$\epsilon_{zz,i}$	Axial strain for i-th layer [-]
$\sigma_{rr,i}$	Radial stress distribution for i-th layer [Pa]
$\sigma_{\phi\phi,i}$	Tangential stress distribution in azimuthal angle direction for i-th layer [Pa]
$\sigma_{zz,i}$	Axial stress distribution for i-th layer [Pa]
I_i	$=-[E_i\alpha_i/(1-\nu_i)]\int_{r_{i-1}}^{r}\theta_i r dr$ [m^2 Pa]
β_i	$=(1+\nu_i)(1-2\nu_i)/E_i$ [Pa^{-1}]
λ_i	$=-(1+\nu_i)/E_i$ [Pa^{-1}]
C_i	Integration constant for i-th layer
D_i	Integration constant for i-th layer
φ_i	$=\nu_i\epsilon_{zz}/\beta_i$ [Pa] for cylinder
p_i	Radial contact pressure at surface/interface points [Pa]
γ_i	$=r_{i-1}^2/r_i^2$ [-] for cylinder
S_i	$=\gamma_i\gamma_{i+1}(\lambda_i-\beta_{i+1})+(\lambda_{i+1}-\lambda_i)\gamma_i$ [Pa^{-1}]
G_i	$=\lambda_{i+1}-\beta_i+(\beta_i-\beta_{i+1})\gamma_{i+1}$ [Pa^{-1}]
c_i	Recursive relation; Defined by Eq. (49) [-]
d_i	Recursive relation; Defined by Eq. (50) [-]

References

[1] Matos, C.R., Carneiro, J.F., & Silva, P.P., Overview of Large Scale Underground Energy Storage Technologies for Integration of Renewable Energies and Criteria for Reservoir Identification, *Journal of Energy Storage*, 21, 2019, 241-258.
[2] Li, X. Zhang, Y. Fan, X & Yin. J., Impact of Substitution Rate on Energy Consumption Structure: A Dynamical System Approach, *Arabian Journal for Science and Engineering*, 46, 2021, 1603-1615.
[3] Acar, C., & Dincer, I., Review and evaluation of hydrogen production options for better environment, *Journal of Cleaner Production*, 218, 2020, 835-849.
[4] Abdalla, A.M., Hossain, S., Nisfindy, O.B., Azad, A.T., Dawood, M., & Azad, A.K., Hydrogen production, storage, transportation and key challenges with applications, A review, *Energy Conversion and Management*, 165, 2018, 602-627.
[5] Breeze, P., *Power System Energy Storage Technologies*, Academic Press, 2018.
[6] Tarkowski, R., Underground hydrogen storage: Characteristics and prospects, *Renewable and Sustainable Energy Reviews*, 105, 2019, 86-94.
[7] Azzuni, A., & Breyer, C., Energy security and energy storage technologies, *Energy Procedia*, 155, 2018, 237-258.
[8] Colbertaldo, P., Agustin, S.B., Campanari, S., & Brouwer, J., Impact of hydrogen energy storage on California electric power system: Towards 100% renewable electricity, *International Journal of Hydrogen Energy*, 44(19), 2019, 9558-9576.

[9] Andersson, J., & Grönkvist, S., Large-scale storage of hydrogen, *International Journal of Hydrogen Energy*, 44(23), 2019, 11901-11919.
[10] Foh, S., Novil, M., Rockar, E., & Randolph, P., Underground hydrogen storage, *Final report Salt caverns, excavated caverns, aquifers and depleted fields*, 1979.
[11] Kruck, O., Crotogino, F., Prelicz, R., & Rudolph, T., *Overview on all Known Underground Storage Technologies for Hydrogen*, EU, 2014.
[12] Teodoriu, C., Ugwu, I.O., & Schubert, J.J., Estimation of Casing-Cement-Formation Interaction using a new analytical model, *SPE EUROPEC/EAGE Annual Conference and Exhibition*, Barcelona, Spain, 2010.
[13] Boukortt, H., Amara, M., Hadj Meliani, M., Bouledroua, O., Muthanna, B.G.N., Suleiman, R.K., & Pluvinage, G., Hydrogen embrittlement effect on the structural integrity of API 5L X52 steel pipeline, *International Journal of Hydrogen Energy*, 43(42), 2018, 19615-19624.
[14] Arthur, J.D., Understanding Mechanical Integrity Testing and Underground Gas Storage: The Key to Success. Presentation, *Ground Water Protection Council's 2017 Annual Forum*, 2017.
[15] Bromhal, G., Well Integrity for Natural Gas Storage in Depleted Reservoirs and Aquifers, *Office of Fossil Energy*, 2016
[16] Bai, M., Song, K., Sun, Y., He, M., Li, Y., & Sun, J., An overview of hydrogen underground storage technology and prospects in China, *Journal of Petroleum Science and Engineering*, 124, 2014, 132 – 136.
[17] Xie, J., Matthews, C., & Dessein, T., Finite Element Analysis for Understanding Oil and Gas Well Deformation Mechanisms, *SIMULIA: Science in the Age of Experience*, 2016.
[18] Manceau, J.C., Tremosa, J., Lerouge, C., Gherardi, F., Nussbaum, C., Wasch, L.J., & Claret, F., Well integrity assessment by a 1:1 scale wellbore experiment: Exposition to dissolved CO2 and overcoring, *International Journal of Greenhouse Gas Control*, 54, 2016, 258-271.
[19] Shi, Y., Li, B., Guo, B., Guan, Z. & Li, H., An Analytical Solution to Stress State of Casing-Cement Sheath-Formation System with the Consideration of its Initial Loaded State and Wellbore Temperature Variation, *International Journal of Emerging Technology and Advanced Engineering*, 5(1), 2015, 59-65.
[20] Zhang, H., Shen, R., Yuan, G., Ba, Z., & Hu, Y., Cement sheath integrity analysis of underground gas storage well based on elastoplastic theory, *Journal of Petroleum Science and Engineering*, 159, 2017, 818-829.
[21] Bai, M., Song, K., Li, Y., Sun, J., & Reinicke, K.M., Development of a Novel Method To Evaluate Well Integrity During CO2 Underground Storage, *SPE Journal*, 20(03), 2015, 628-641.
[22] Song, C. L., & Dan, Y., Stress Analysis of the Underground Gas Storage Well Stored CNG Based on the Finite Element Method, *Advanced Materials Research*, 704, 2013, 338-342.
[23] Bakaiyan, H., Hosseini, H., & Ameri, E., Analysis of multi-layered filament-wound composite pipes under combined internal pressure and thermomechanical loading with thermal variations, *Composite Structures*, 88, 2009, 532-541.
[24] Lou, M., Wang, Y., Tong, B., & Wang, S., Effect of temperature on tensile properties of reinforced thermoplastic pipes, *Composite Structures*, 241, 2020, 112119.
[25] He, Y., Vaz, M. A., & Caire, M., Stress and failure analyses of thermoplastic composite pipes subjected to torsion and thermomechanical loading, *Marine Structures*, 79, 2021, 103024.
[26] Yeo, W.H., Purbolaksono, J., Aliabadi, M. H., Ramesh, S., & Liew, H.L., Exact solution for stresses/displacements in a multilayered hollow cylinder under thermo-mechanical loading, *International Journal of Pressure Vessels and Piping*, 151, 2017, 45-53.
[27] Vedeld, K., & Sollund, H.A., Stresses in heated pressurized multi-layer cylinders in generalized plane strain conditions, *International Journal of Pressure Vessels and Piping*, 120-121, 2014, 27-35.
[28] Hartmann, S., Mohan, J., Müller-Lohse, L., Hagemann, B., & Ganzer, L., An analytical solution of multi-layered thick-walled tubes in thermo-elasticity with application to gas-wells, *International Journal of Pressure Vessels and Piping*, 161, 2018, 10-16.
[29] Incropera, F.P., & David, P. D., *Introduction to heat transfer*, John Wiley & Sons, 2011.
[30] Hetnarski, R.B., *Encyclopedia of Thermal Stresses*, Springer, Netherlands, 2014.
[31] Boresi, A.P., & Schmidt, R. J., *Advanced Mechanics of Materials*, 6th Ed, Wiley, India, 2009.
[32] NORSOK D-010, *Well integrity in drilling and well operations*, Norway, 2004.
[33] Michanowicz, D.R., Buonocore, J.J., Rowland, S.T., Konschnik, K.E., Goho, S.A., & Bernstein, A.S., A national assessment of underground natural gas storage: identifying wells with designs likely vulnerable to a single-point-of-failure, *Environmental Research Letters*, 12(6), 2017, 064004.

ORCID iD

Lih Chi Sim https://orcid.org/0000-0001-7444-901X
Wei Hong Yeo https://orcid.org/0000-0001-6175-3370
Judha Purbolaksono https://orcid.org/0000-0002-7467-4329
Lip Huat Saw https://orcid.org/0000-0001-6467-0239
Jing Yuen Tey https://orcid.org/0000-0002-9888-0397
Jer Vui Lee https://orcid.org/0000-0003-4870-8772
Ming Chian Yew https://orcid.org/0000-0002-1883-9723

How to cite this article: Sim L.C. et al., Thermomechanical Stresses of Multilayered Wellbore Structure of Underground Hydrogen Storage – A Simplified Solution Based on Recursive Algorithm, *J. Appl. Comput. Mech.*, 8(4), 2022, 1287–1298. https://doi.org/10.22055/jacm.2022.39453.3411